Landfill side slope lining system performance: A comparison of field measurements and numerical modelling analyses

Katarzyna A. Zamara
CICE, School of Civil and Building Engineering, Loughborough University LE11 3TU, UK
& FCC Environment Ltd Ground Floor West, 900 Pavilion Drive, Northampton, NN4 7RG
Katarzyna.Zamara@FCCEnvironment.co.uk
Neil Dixon & Gary Fowmes
School of Civil and Building Engineering, Loughborough University, LE11 3TU, UK.
N.Dixon@lboro.ac.uk
D. Russell V. Jones & Bo Zhang
Golder Associates (UK) Ltd Nottingham, NG12 5BL, UK. R.Jones@golder.com

Abstract

Low permeability engineered landfill barriers often consist of a combination of geosynthetics and mineral layers. Even though numerical modelling software is applied during the landfill design process, a lack of data about mechanical performance of landfill barriers is available to validate and calibrate those models. Instrumentation has been installed on a landfill site to monitor multilayer landfill lining system physical performance. The lining system comprises of a compacted clay layer overlaid by high density polyethylene geomembrane, geotextile and sand. Data recorded on the site includes: geosynthetic displacements (extensometers), strains (fibre optics, Demec strain gauges, extensometers) and stresses imposed on the liner (pressure cells). In addition, temperature readings were collected by a logger installed at the surface of the geomembrane, at the clay surface using pressure cell thermistors and air temperature using a thermometer. This paper presents readings collected throughout a period of three years and compares this measured performance with the corresponding numerical modelling of the lining system for stages during construction. Numerical modelling predictions of lining system behaviour during construction are comparable with the measurements when the geosynthetics are covered soon after placement, however where the geosynthetics are left exposed to the sun for an

extended period of time, *in situ* behaviour of the geosynthetics cannot be replicated by the numerical analysis. This study highlights the significant influence of the effect of temperature on geosynthetics displacements. A simple thermal analysis of the exposed geosynthetics is used to support the explanation for observed behaviour.

Key words: landfill lining system, geosynthetics, monitoring, numerical modelling.

1 INTRODUCTION

Geosynthetics are materials that have been widely used in the construction industry for decades. More importantly, they have been recognised as a suitable material for waste barriers and have become extensively applied in landfill engineering. Even though their *in situ* mechanical behaviour has not been fully measured or defined, experience gained through multiple applications and ease of installation has resulted in their acceptance by regulatory agencies, designers and contractors. For over two decades geosynthetic interface shear strength has been a subject of investigations throughout the world. Dixon *et al.* (2006) present data from 76 sources of interfaces commonly deployed in landfills. Furthermore, developed methods of measurement, the procedures and variability in obtainable results are still the subject of many on-going discussions. To consider the complex nature of material behaviour and their interactions, landfill design methods incorporating geosynthetic materials can take the form of limit equilibrium or advanced numerical modelling analyses. The latter are often used for more complicated design cases, where the *in situ* conditions are not favourable and/or serious environmental implications would result from failure. Even though the number of designs based on numerical modelling has increased in recent years, very limited field data on in service performance of lining systems exists to allow validation of models in order to confirm their accuracy and suitability. Often, model verifications are based on analysis of landfill failures (Koerner and Soong 2000, Dixon

and Jones 2003, Muhsiung 2005) but these cannot deliver data on in service performance of the materials and composite lining systems such as: displacements, strains or tensile stresses in geosynthetic components resulting from overburden pressures, process of waste placement during landfill cell filling and long term degradation of the waste body. Therefore, lining system stability (ultimate limit state related to large scale movements) and integrity (serviceability limit state - overstressing of liner elements and subsequently loss of original functions) in terms of construction safety, optimal and reliable design (accurate prediction of imposed stresses, evaluation of strains and axial forces within geosynthetics) are still topics of research.

Since only limited information exists on *in situ* geosynthetic performance in the landfill environment, the need for numerical model validation and calibration is self-evident. Dixon *et al.* (2012) summarises the current state of research on lining system stability and integrity, and emphasises common engineering problems related to geosynthetics in the landfill environment (*i.e.* staged construction, strain softening interfaces, progressive failure, tensile stresses in materials, representation of waste parameters and behaviour, ageing and waste biodegradation). The purpose of the study reported by Dixon *et al.* (2012) was to investigate interface strain softening design issues, as often interfaces between materials installed on landfill slopes (geosynthetics/geosynthetics, geosynthetics/soil) reveal strain softening behaviour (*i.e.* the interface shear strength decreases to residual large displacement values after reaching its peak). Studies have been carried out to investigate these phenomena, to incorporate these aspects in numerical analyses (*e.g.* Arab 2011, Sia & Dixon 2012, Fowmes *et al.* 2005) and some limited number of physical experiments have been carried out (*e.g.* Villard *et al.*1999, Fowmes *et al.* 2008). However data to verify actual *in situ* behaviour of lining components and their interfaces when subject to staged construction and waste settlement is still inadequate.

This paper presents results from a three year full scale investigation of mechanical performance of a multi-layered landfill lining system, carried out at the Milegate Extension Landfill, UK. The lining system comprises a compacted clay layer, overlaid by geomembrane, geotextile and a sand layer. The project started in June 2009 and monitoring was carried out for the following 3 years. Instrumentation installed on the site consists of pressure cells (PC), extensometers (Ext), fibre optic strain gauges (FO), Demec strain gauges (DSG) and additionally thermometers.

This paper aims to provide improved understanding of lining system *in situ* behaviour and to highlight factors that influence interface mobilised strength and geosynthetic strains. A numerical model representing the configuration and construction sequence of a side slope at the Milegate landfill, was created to validate and calibrate the numerical modelling design approach. Numerical analyses were undertaken using FLAC software and the results compared with the measured *in situ* behaviour of the lining system materials. Analyses were carried out to replicate common design conditions including staged construction, a multiple mineral/geosynthetic lining system with associated multiple strain softening interfaces, and waste body compression during filling under self-weight.

2 MILEGATE EXTENSION LANDFILL STUDY CASE

Details regarding the site monitored such as: slope geometry, instrumentation and its performance, installed lining materials and history of construction works undertaken are reported by Zamara *et al.* (2012). Only a brief description of the main aspects of the site works is reported below as an introduction.

100 *2.1 The trial site*

101 The monitored slope has a length of 31.2 m and height of 16 m with an inclination angle of
102 1v:2.5h (~21.8°). Figure 1 shows the site location, slope geometry and photographs of initial and
103 one of the final waste placement stages. The lining system deployed was placed in addition to the
104 pre-existing clay liner, and therefore is an additional and hence sacrificial layer that does not
105 form part of the approved containment system at this site. The combination of materials forming
106 the lining system was: clay, geomembrane, geotextile and a veneer of soil, which were chosen to
107 represent common practice.

108 *2.2 Materials*

109 The instrumented lining system comprised of a 2 mm double textured HDPE geomembrane 5 m
110 wide panel, with density of 0.949 g/cm^3 (GM TMT from Atarfil S.L.) placed on top of the
111 compacted 1.0 m thick clay liner with a maximum permeability of 1x10^{-9} m/s . The
112 geomembrane was overlain by a non-woven needle punched geotextile 5m wide panel. This
113 protection layer has a static puncture strength [CBR] of 14 kN, thickness of 7.8 mm and weight
114 of 1400 g/m^2 (HPS14 from GeoFabrics Ltd.). The multilayered landfill system is shown
115 schematically in Figure 2. The geomembrane and geotextile were anchored in a "U" shaped
116 600mm x 600mm anchor trench at the top of the slope. The geomembrane/geotextile
117 "experimental" panel replaced the existing geocomposite drainage material over a slope width of
118 5.0 m. A nominally 0.5 m thick sand veneer was placed in stages on the geotextile ahead of
119 waste placement. This represents common practice of providing a mineral drainage layer on side
120 slopes. Prior to waste placement the sand layer was placed in lifts parallel to the slope along 10
121 m of slope length. When the waste body reached the top of the first veneer a second 10 m sand
122 layer measured parallel to the slope was placed along the slope. When the waste reached the top
123 of the second veneer layer a third and last veneer lift was constructed and the whole length of the

slope was then covered with a 0.5 m thick sand layer. Placement of the sand veneers provided an opportunity to measure response of the underlying geosynthetic components to the applied load. In practice sand is not used for drainage layers due to its fine grading, relatively low permeability and susceptibility to clogging but it was used in this study to produce loading equivalent to gravel typically used for mineral drainage layers.

2.3 Summary of instrumentation

Instrumentation was designed to measure parameters that are the most important for the design process and hence long term performance of the lining system. The instrumentation delivers information about stresses imposed on the liner (three pressure cells along the slope at the clay/ geomembrane interface), displacements of the geosynthetic liner elements and relative displacement between the liner elements (extensometers located on the geomembrane and geotextile), strains in the geomembrane (measured using Demec strain gauges, Fibre optic cables and calculated from extensometers) and geotextile strains (calculated from extensometers). Figure 3 presents the schematic location of the instruments along the slope, and Table 1 details the type, number and measured parameters of instrumentation installed on the site. Full details of the instrumentation selection, installation and operation is provided by Zamara *et al.* (2012)

3 MILEGATE EXTENSION LANDFILL NUMERICAL MODELLING

One of the main aims of the study was to validate the numerical modelling results for performance of the lining system during construction and waste placement against measured *in situ* behaviour of the lining system. It was planned to fill the cell where the monitored slope was located with waste within 1-2 years after the instrumentation installation, however this process was delayed due to the current economic situation, which resulted in slower filling rates and hence prolonged exposure of the lining materials to atmospheric conditions.

148 *3.1 Finite Difference Computer Software*

149 A commercial software program FLAC (Itasca International Inc.) was used to compute
150 predicted behaviour of lining materials and interfaces on the monitored landfill slope. FLAC has
151 been used in several previous landfill geotechnical engineering studies (*e.g.* Fowmes *et al.* 2005,
152 Arab 2011, Sia & Dixon 2012). The code allows materials that undergo large strains to be
153 modelled, and hence it is appropriate for use in studies of landfill construction processes. It can
154 represent waste body deformation, interface displacement and geosynthetic strains. FLAC
155 analyses reported in this paper were based on a landfill design procedure developed by Fowmes
156 *et al.* (2007).

157 *3.2 The Landfill Model Geometry - general*

158 The model was built to represent the major aspects of the cell construction and waste filling
159 process. The cell was formed from a clay layer modelled at the cell slope and base. The model
160 allowed representation of staged construction of each sand veneer stage (0.5 m thick sand veneer
161 was placed in 3 lifts, in 10 m long layers measured parallel to the slope), followed by 4 waste
162 lifts. In total the model computes 16 stages of material placement (1st clay, 2nd sand veneer, 3-
163 6th waste lifts, 7th sand veneer, 8-11th waste lifts, 12th sand veneer, 13-16th waste lifts). Each
164 waste lift has a vertical thickness of approximately 1 m.

165 *3.3 Multilayer lining system*

166 The geosynthetic lining elements were placed along the clay slope. Since the *in situ* material
167 comprised of well compacted clay over a strata with high strength and stiffness properties, clay
168 behaviour was not monitored and for the modelling approach it was considered to provide a
169 stable foundation for the lining system. It should be noted that initially high stiffness values were
170 assumed for the clay (150 MPa) as no movement was expected within the compacted clay layer,
171 however, in further sensitivity analyses the clay stiffness was reduced to investigate the influence

on geomembrane displacements (50 MPa). The geosynthetics were modelled as elastic beam elements anchored at the top of the slope. Three interfaces between lining components were assigned: clay/geomembrane, geomembrane/geotextile, geotextile/sand, and additionally the sand/waste interface was given waste properties. Information on geosynthetic tensile behaviour was provided by the suppliers of the materials: geomembrane thickness was 2 mm and Young secant modulus E= 338 MPa (for 5% strain), geotextile thickness was 7.8 mm and Young modulus E=120 MPa (for 5% strain). Geosynthetics were not expected to fail through excessive tensile deformations (latterly proven by both field measurements and results from the analyses), therefore secant modulus values for 5% strain were used to generate conservative strains.

Soil and waste materials where represented by Mohr –Coulomb failure criterion and the properties assigned to the materials are given in Table 2. Waste properties are based on data available from the literature (Jones & Dixon 2005).

3.4 Interfaces

The importance of interface strength parameters has been emphasised previously by various authors (*e.g.* Filz *et al.* 2001, Jones & Dixon 2005). In general it is accepted that landfill side slope lining systems might undergo interface shear strength softening behaviour and therefore the Milegate model in FLAC incorporated strain softening interfaces between each lining element. Interface shear strengths for each combination of materials were measured in a direct shear box machine in a laboratory test programme and used in the numerical analyses (Table 3). For each interface tests were carried out with five different normal stresses: 10, 25, 50, 100 and 200 kPa. In order to acquire detailed information on the interfaces, tests were carried out with the following conditions: dry interfaces (soil/geotextile, geotextile/geomembrane, geomembrane/clay), submerged interfaces (soil/geotextile, geotextile/geomembrane), and slow

displacement rate in an attempt to reflect drained conditions (geomembrane/clay). Each test was repeated at least three times using new materials. Waste/soil interface properties were not investigated in the laboratory and the values used are based on the common approach of assigning the waste material properties to its interface with the granular drainage layer. In addition, a key element of the model was the availability of strain softening interface behaviour following the approach developed by Fowmes *et al.* (2007).

3.5 The modelling process

The most comprehensive and consistent site data was delivered from the extensometer measurements of geomembrane and geotextile displacements, hence the first attempts to compare numerical modelling outputs with the site data were initially focused on geosynthetic displacements and the numerical model was then developed in an iterative process. One by one sub-procedures were added to the basic model and examined in terms of generated geosynthetic displacements during construction and waste placement. In the study four different interface shear strength property scenarios were investigated: peak, residual, strain softening and reduced values in an attempt to replicate the measured material displacements. Additionally, stiffness values for the clay liner, geotextile and sand were reduced systematically in an attempt to reproduce monitored lining system behaviour. These reduced values could be justified as resulting from potential material and interface degradation processes.

4 COMPARISON OF MEASURED AND MODELLED BEHAVIOUR

4.1 Stresses imposed on the liner

Computed values of pressures imposed on the liner are within the ranges recorded on the site using pressure cells (Figure 4). It can be concluded that stresses imposed on the side slope lining

system, from waste unit weight and sand veneer can be represented by the numerical model. Time has not been explicitly considered in the numerical analysis but stages of construction are defined. The reference point for the plotted, measured and modelled values is the waste height above the landfill base. The site records have been plotted against time to provide the time framework for this study and to present the cell filling time-line.

The two lower pressure cells included thermistors measuring temperature at the clay surface (Figure 3 PC24, PC30) and this facilitated temperature correction of the pressure cell readings, which are plotted in Figure 4. It can be noticed that once the pressure cells were covered with waste, temperatures on the clay surface show significantly less variation, and winter clay temperatures did not decrease significantly from summer values.

4.2 Geosynthetic deformations from extensometer readings vs. modelling predictions

Figure 5 presents an overview of all the displacements recorded by extensometers attached to the geomembrane and geotextile throughout the three year construction and waste filling period. Additionally, Table 4 summarises the maximum displacements of the geomembrane and geotextile computed for various configurations of in-put parameters; Displacement values recorded on the site are included in Table 4 for comparison.

4.2.1 Geotextile behaviour

Significant movements of the geotextile were recorded. Extensometers located within the middle and upper parts on the slope recorded displacement up to 80 mm down slope. These large movements were triggered mostly at the time of the second sand veneer placement. It can be observed that site measurements show less consistent (along the slope) and more localised displacements than the computed simulations.

241 Results from the series of FLAC analyses are compared with the measured behaviour in Figures
242 5 to 8. The simulation labelled “MIN” uses input parameters that give the lowest displacements
243 of the lining components. These simulations were undertaken using a basic model with interfaces
244 described with either peak or residual shear strength properties (*i.e.* the interfaces are not strain
245 softening). Computed results using peak and residual interface strengths were comparable as
246 peak strength was not exceeded along the interface. “MAX” uses worst (*i.e.* lowest) credible
247 interface shear strength properties and reduced clay stiffnesses - assuming softening of clay after
248 placement on the slope. Using these parameters, unsurprisingly, computed displacements are the
249 highest obtained. Analyses using the current best practice approach, as defined by Fowmes *et al.*
250 (2007) are defined as “_Best_Practice” simulations. These analyses incorporate strain softening
251 interfaces between lining elements and use the measured, unaltered, material parameters.

252 Numerical modelling results using the basic approach produced limited agreement with the
253 measured behaviour, especially in terms of geotextile displacements (Figure 5 Geotextile MIN
254 plot). In general for the standard approach it was not possible to replicate geotextile movements
255 in the middle and top sections of the slope, with the largest movement in the model occurring
256 within the toe section. It can be noticed that the geotextile did not deform in a manner modelled.
257 Model output displacements are regular, with predictable trends that increase steadily until the
258 final stage of loading. However, on the site no significant movements occurred once the slope
259 was covered by the second sand veneer. Furthermore, results for the geotextile are in a good
260 agreement for the lower section of the slope where the geotextile was covered by the sand
261 veneer, and which was not left exposed for an extended period of time. Although behaviour
262 during staged construction is not well replicated, the final total displacements computed in the
263 range of 30mm for the lower section of the slope are consistent with the monitored values. For

the top section of the slope, geotextile *in situ* displacements are comparable to the computed ranges only when the values of interface shear strength of the lining components are reduced significantly (*e.g*. MAX analysis shown in Figure 7). In the MAX analysis the geomembrane movement is increased by assuming softening of the clay, thus reducing stiffness, and the geotextile stiffness is increased to replicate the possible effects of weathering (Lodi *et al*. 2008). The MAX analysis represents reasonably well the measured behaviour of the section of geotextile that was exposed for an extended period (*i.e.* between placement of the first and second sand veneers), however displacements within the lower sections are significantly overestimated. The "Best_Practice" analysis is able to replicate behaviour of the geotextile for the lower part of the slope length that was rapidly covered by the sand veneer.

Figure 6a-c present plots of selected analyses outputs versus site derived data, for each stage of cell filling for three locations on the slope (*i.e*. extensometer locations: 8.4, 13.8 and 24.6 m below the crest). The main movement for the upper section occurred directly before and during placement of the second sand veneer. In the MAX analysis geotextile movements occur only when the loading is placed directly over the geotextile (*e.g*. top extensometer at location 8.4m records increased movement when the 3rd veneer is constructed (Figure 6a); middle extensometer at 13.8 m when 2nd veneer is placed (Figures 6b); and toe extensometer at 24.6 m due to 1st veneer placement (Figures 6c)). The highest displacements of the geotextile occurred in response to placement of the 2nd sand veneer.

4.2.2 Geomembrane behaviour

Measured geomembrane displacements gradually increased during filling at all locations, but with only limited displacement caused directly by placement of the sand veneers. Maximum displacement reached 25.9 mm within the middle section, but in general the extensometers recorded displacements of 10-20 mm within the geomembrane panel. No significant correlation was found between geotextile and geomembrane locations on the slope with increased displacements.

Geomembrane displacements are represented by the numerical model with relatively good agreement. While the MAX analysis overestimates geomembrane displacements, MIN and "Best_Practice" (Figure 7) both represent the trend and magnitude of monitored values, although values are underestimated in the lower section. For analyses using the "stiffer" clay properties (150 MPa), not much difference in geomembrane movement was observed between the results for the peak, residual, strain-softening and reduced interface shear strength approaches (Table 4).

4.2.3 Summary

Figure 7 presents measured and modelled displacement distributions for the geotextile and geomembrane along the slope, after the final stage of construction. These plots highlight the significant differences in computed geotextile and measured final displacement distributions. The computed maximum geomembrane displacements for the basic analysis (MIN) are in the range of the monitored values but the location of the maximum geomembrane movements differ. Considering behaviour during staged construction (Figures 6a-c) it can be observed that the basic analysis is sufficient to replicate the geomembrane behaviour, however for all instrumented locations the geotextile deformations are underestimated by the basic analysis.

Simulations using peak and residual interface shear strengths gave very similar results. For the basic simulation (MIN), the maximum computed geomembrane displacement is within the range of monitored geomembrane displacements (*i.e.* 20 mm) , although the location of its occurrence is not well represented in the model This behaviour is consistent with the expectation that mobilised strengths are below peak values for shallow slopes such as investigated in this study.

For the geotextile, difficulty was experienced trying to model the exposed section of the material in the upper part of the slope, while the part that was covered by the sand veneer within a few months of liner construction is relatively well modelled using the strain – softening approach (Best_Practice). Due to the complex measured behaviour of the geosynthetics and variability of the conditions they were exposed to, it is difficult to select a "best fit" analysis for the whole slope, as none of the models can reproduce measured behaviour at all areas of the slope in each construction stage. The "Best_Practice" model using measured and best estimate parameters, produced the most consistent fit with observed deformation of the geomembrane and for the lower section of geotextile that was rapidly covered by the sand veneer.

4.3 Strains in the geomembrane imposed by the veneer and waste loading vs. model predictions

Strains in the geomembrane were measured using three independent methods: Demec strain gauges with reading points installed at the top and middle slope sections, fibre optic sensors located in the middle and bottom slope sections (all the sensors were lost prior to the 3rd veneer placement) and extensometers covering the entire slope length. Demec gauges were used to measure strains over a relatively short gauge length of 20 cm. Three measurement positions across the width of the geomembrane panel were located at the slope crest and one position on the panel centreline in the middle of the slope. Extensometer readings can be used to calculate strains but this information is low resolution as measuring points installed on the geomembrane

are a 5.4 m apart, hence strains are average values over this gauge length and only provide low resolution information. The fibre optic sensors provide measurements of average strains over a 1 m long gauge length orientated parallel to the slope. Strain measurements are compared at three stages of construction: after placement of the 1st sand veneer, just prior to placement of the 2nd sand veneer and the final stage after completion of waste filling. For comparison, average values for the measurement sections have been obtained from the model outputs. Monitored and modelled strains in the geomembrane are presented in Figures 8a-c for locations at the top, middle and bottom of the slope. The accuracy, resolution and hence reliability of strain measurements using the different approaches are discussed by Zamara *et al.* (2012). Despite some issues with reliability and reproducibility of measured values, it is considered that the magnitude of the strains is given and comparison of measurements obtained using the different techniques provides confidence in observed trends.

General trends of measured and modelled strains can be identified. The modelling gives compressive strains for the toe section throughout the cell filling stages, while tension in this section was measured on site. This is due to the fact that the toe of the geomembrane moved the most due the presence of a compressible shredded tyre basal drainage layer at the toe of the slope), while the model gives peak displacements at a position 25 m below the slope crest (*i.e.* 6 m above the toe). The middle section experienced a constant tension state and this is replicated in the model although it is underestimated in the basic analysis. Strains computed for the top section are in tension throughout the filling stages and this agrees with Demec strain gauge readings. The extensometer records give compressive strains in the top slope section throughout almost all the stages of construction. This is suspected to be related to temperature effects on the extensometer wires that were difficult to correct and hence there is lower confidence in these measurements. For the final stages only the extensometer readings are available and the accuracy

of these is limited as outlined above. In general, the model gives the same strain trends but different magnitudes.

Strains recorded after placement of the 1st sand veneer

When the toe of the slope was covered by the 0.5m thick sand layer the model indicates geomembrane compression at the toe and tension within the uncovered sections up slope (Figure 8a). However, *in situ* measurements shows that placement of the sand veneer caused tensile strains greater than 0.1% within the loaded sections of the liner and generally smaller (extensometer and fibre optic measurements) tensile strains of 0.06% within the sections above. However, the Demec strain gauge measurements show higher tensile strains in the exposed geomembrane of 0.15% and 0.18% for the crest and middle sections respectively.

Strains recorded just prior to placement of the 2nd sand veneer

Prior to the second veneer most of the instrumentation show tensile strains within the whole length of the geomembrane (Figure 8b). In the toe section the fibre optic measurements reach over 0.7% and for the extensometers over 0.2% while the top and middle sections stay in a range of 0.1-0.2%. The model MAX outputs give uniformly distributed tensile strains of 0.09% for the exposed sections of the slope and indicates compression within the toe region.

Final stage strains following completion of waste filling

After placement of the 3rd sand veneer the Demec gauge measurement locations were no longer accessible and the fibre optic sensors were not operating, and therefore only extensometer readings can be used to provide information on strains. These indicate tensile strains within the middle and lower sections and compression within the top section of the slope. These only agree with the computed values in the middle section of the slope.

Summary

In terms of the ability of the model to represent *in situ* lining component performance, it can be concluded that only general trends of behaviour can be reproduced. Monitored behaviour is more complex and description of all the incorporated factors is beyond the basic analysis. The basic model (MIN) represents the geomembrane behaviour in a very limited way, with underestimated magnitudes of the recorded strains. The highest tensile strains are recorded at the very top point of the slope directly adjacent to the anchor, while instrumentation records increased values within the lower slope sections, with fibre optic measurements reaching 0.7% and extensometer derived values around 0.2% throughout the monitoring period.

Additionally, the model is not able to represent compression/wrinkling/folding behaviour as this is complicated numerically to describe and requires confined compressive parameters for the geosynthetics that are not routinely available.

5 LINER EXPOSED TO ATMOSPHERIC CONDITIONS

It can be observed that the basic numerical analysis underestimates geotextile displacements, hence it can be concluded that the major geotextile displacements occur due to factors which are not represented in the FLAC modelling approach employed. Temperature/solar radiation influences are not commonly considered in the standard design processes for landfill lining systems. Additional analysis was undertaken in an attempt to investigate environmental (*i.e.* temperature) influences on geosynthetic performance. Evidence was discovered on site supporting the hypothesis that HDPE cyclic expansion and contraction caused wrinkle formation in the geomembrane driving associated geotextile deformations. However while the geomembrane contracts in response to reductions in temperature the overlying geotextile material does not recover and this results in formation of permanent wrinkles in the exposed geotextile following series of temperature cycles. The Milegate extensometer measurements

revealed evidence of geomembrane/geotextile interaction and geotextile movement due to HDPE geomembrane thermal deformation occurring within exposed areas of the side slope. The FLAC analyses cannot replicate this mechanism of behaviour.

5.1 Geosynthetics thermal behaviour - overview

It is widely accepted that black geomembrane will absorb heat from the sun. HDPE exposed to atmospheric conditions (*i.e.* solar radiation and high temperature amplitudes) will respond by expanding or contracting, and this will occur in response to daily cycles and seasonal changes in temperature and will result in cyclic wrinkle formation within the geomembrane. Studies of geosynthetic thermal behaviour have been carried out by Giroud and Morel (1992) who introduced a simplified model to describe wrinkle geometry and distribution on a horizontal geomembrane due to thermal expansion/contraction behaviour. However, their procedure has many limitations: the analysis was conducted for a horizontal surface while geomembranes are widely installed on slopes with varying inclinations, the geometry of wrinkles in the geomembrane was simplified and predictions regarding wrinkle occurrence and overall behaviour were not fully considered. Studies regarding thermal behaviour of various geomembranes (*i.e.* Koerner *et al.* 1993, Peltie *et al.* 1994, Cadwallader *et al.* 1993, Ehrenberg & Recker 2012) show the significant influence of geomembrane colour on the magnitude of temperature reached during exposure and hence behaviour (*i.e.* up to 30°C difference between white and black geomembrane). It has been recognised that HDPE surface temperature exceeds, often significantly, monitored air temperature, and depends on the solar radiation (Peltie *et al.* 1994). Moreover, Take *et al.* (2011) have observed that wrinkles have increased temperatures compared to the rest of the HDPE (due to air trapped underneath the wrinkle). Take *et al.* (2012) reported temperatures up to 15°C higher than the unwrinkled HDPE. Additionally, Akpinar &

Benson (2005) report temperature effects on shear strength properties of geomembrane/geotextile interfaces with increased friction angle with elevated temperature and decreased values due to temperature decreases (reported change in interface strength friction parameter was 2-3° for ΔT=33°C). Existing research has focused on wrinkle behaviour when subjected to overburden stresses, as these affect leakage flow.

In this study, the influence of geomembrane wrinkle formation on the overlaying geotextile material is considered important for deformation of the lining system components during construction and waste placement.

While there are extensive studies of HDPE wrinkling, to the authors' knowledge, data available on geotextile wrinkle development in composite geosynthetic lining systems exposed to solar radiation are limited. Lodi *et al.* (2008) investigated geotextile properties exposed to weathering. It was reported that after three months, there was a reduction material tensile strength and mass per unit area, but an increase in tensile stiffness. Information regarding geotextile wrinkle formation, locations, sizes and displacements along the slopes are not well documented.

For this study temperature records for the upper surface of the geomembrane beneath the geotextile (measured at the middle section of the slope) are presented in the Figure 9 for a period of one year while the geosynthetics were exposed at this location. Daily changes in the temperature reach up to ΔT_d=10°C, while seasonal changes are of over ΔT_s=30°C. Air temperature recorded for this area in the same period, revealed seasonal temperature difference of 40°C (WunderGround, 2012). The observed wrinkle formation, HDPE contraction and expansion, and its influence on geotextile deformation is considered to be an important behaviour explaining mechanisms of recorded increased displacements of the geotextile.

449 *5.2 Discussion on thermal factors*

450 Based on observations and measurements at Milegate it is concluded that prolonged exposure to
451 solar radiation has a significant influence on geosynthetic lining system performance. The upper
452 section of the slope remained uncovered, and hence exposed, from installation in July 2009 until
453 October 2011). Geomembrane deformations due to seasonal temperature changes are shown by
454 the Demec strain gauge measurements made at the top and across the slope (Figure 10), and
455 these deformations are also detected by the extensometer deformation measurements. Cyclic
456 daily deformations were not directly monitored; however changes in geomembrane and
457 geotextile wrinkling over a period of hours were observed during site visits. Wrinkles were
458 documented in site photographs (*e.g.* Figure 11). It is considered that geomembrane seasonal
459 thermal expansion was reproduced by the overlying geotextile. The geomembrane was installed
460 during the summer time (*i.e.* during a period of high temperatures), hence expansion would be at
461 or close to maximum. Because the geomembrane is anchored, as is the geotextile, at the top of
462 the slope, temperature decrease towards the first winter season would result in material
463 contraction, which is represented by readings from extensometers Ext1 and Ext2, which
464 demonstrate small movements up slope. Non-woven geotextile contracts only a small amount
465 when temperatures drop and hence although wrinkles in the geomembrane disappeared in
466 periods of low temperature, those in the geotextile did not. Figure 11 shows a geotextile wrinkle,
467 which is not supported underneath by a geomembrane wrinkle. Although geomembrane wrinkle
468 formation is replicated by the geotextile, the shrinking of wrinkles is not.

469 In a simplified evaluation of the geosynthetic thermal *in situ* behaviour, HDPE thermal
470 expansion was calculated for two coefficients: 1.1×10^{-4}cm/cm/°C (Koerner 2005) and 1.5×10^{-4}cm/cm/°C (Sheirs 2009) in conjunction with ranges of temperature seasonal changes recorded
471

directly on the site (ΔT_s = 30°C, Figure 9), and in the region (ΔT_s = 40°C, WunderGround, 2012). The results of this simplified analysis are presented in Table 5 where they are compared with the down slope deformations of the geotextile measured during placement of the 2nd sand veneer. It can be seen that these are comparable. It is concluded that existence of wrinkles in the exposed section of geotextile allowed rapid downslope displacements to occur during loading from the sand. This resulted in relative shear displacements between the geomembrane and geotextile and has implications for mobilisation of interface shear strength and hence for stability of the side slope lining system.

6 PROJECT LIMITATIONS/COMMENTS

Considerable effort was expended to ensure selection of appropriate instruments and correct installation that would provide reliable and consistent measurements. Nevertheless it is acknowledged that the study has several limitations:

- All the instruments were subjected to temperature changes and hence thermal corrections are required. These were based on the coefficients available from the literature (details are presented in Zamara *et al.* 2012), but it is noted that thermal calibration of the materials and instruments is a challenging task;
- Extensometer readings represent localised movement of the six attachment points on the geomembrane and geotextile and these may not adequately reflect the behaviour of the entire material sheets (*i.e.* wrinkle formation);
- Strains calculated from extensometer records are averaged over 5.4m gauge lengths and therefore average local behaviour;

- Geomembrane strain information acquired from the fibre optic sensors are more comprehensive as the sensors were installed at 1m gauge lengths along the geomembrane, however sensors were lost due to damage throughout the project and therefore no readings are available after placement of the 3rd sand veneer;
- Most of the instrumentation was installed along the centre line of the panel and plane strain conditions are assumed, however the field trial was only one panel wide, thus lateral strain may have occurred; and
- Additionally, it is recognised that validation of numerical modelling design approaches currently in use would benefit if more of this type of monitoring data was available, particularly for different lining system configurations, slope geometries and with consideration given to various rates of waste placement, not only in terms of geosynthetics loadings but also lengths of time the lining exposure to atmospheric conditions.

7 CONCLUSIONS

The Milegate Extension Landfill monitoring project was conducted for three years. The initial aim was to validate standard design approaches incorporating numerical modelling and to better understand mechanisms affecting lining system in-service performance.

The Milegate study provides information on the lining system performance before and during waste placement, which is presented here, and it is planned to conduct further monitoring after landfill closure as waste degradation and settlement occurs. Collected data included: stresses imposed on the lining system, geosynthetic displacements, geosynthetic strains and temperature and these are presented in the paper. Numerical modelling of the monitored slope was conducted

using a range of material models and ranges of key parameters. Selected analyses using FLAC are presented in this paper and compared with the site measurements.

Monitoring revealed that exposed sections of geotextile experienced significant displacements. This behaviour of the lining system could not be replicated using a numerical model. However, current best practice modelling is able to reproduce observed behaviour of the lining components when they are covered and hence not subject to cycles of temperature driven by solar radiation. It is concluded that the observed geotextile displacements that occurred during placement of the 2nd sand veneer are a result of the presence of irrecoverable wrinkles in exposed areas of the slope driven by thermal expansion of the underlying geomembrane. It is acknowledged that the influence on composite liner behaviour of prolonged exposure to weather conditions is currently poorly understood. In an attempt to replicate this behaviour, analyses were conducted using reduced values of the lining system interface shear strength and modified soil and geotextile material properties (*i.e.* reduced interface shear strength of the lining components reflecting wrinkling of the exposed materials and ageing of the geosynthetics) but this approach was not able to reproduce measured displacements .

It should be emphasised that for the section of slope covered by the sand veneer, where the geosynthetics are not directly exposed to solar radiation, displacement values computed using a standard modelling approach are comparable to measured values. This indicates that standard numerical modelling approaches are not applicable when prolonged expose of the geosynthetics and thermal effects become the dominant mechanism controlling displacements.

It is uncommon to consider temperature effects on performance of geosynthetic based landfill side slope liner systems as this is significantly more complicated than the standard design approach. However, attempts should be made to assess the likely influence of cycles of

temperature on performance if it is expected that the liner will be left uncovered for a prolonged period of time due to slow filling rates. Relative displacement between the geotextile and geomembrane can result in mobilisation of post peak interface shear strengths and hence reduced stability that could lead to uncontrolled slippage of the liner and overlying waste. It is advised that if geosynthetics might be exposed to weathering for a prolonged time, reduced values for interface shear strength, and modified values for materials properties, should be considered in design.

ACKNOLEDGEMENTS

EPSRC, CICE at Loughborough University and Golder Associates UK Ltd funded Engineering Doctorate student Katarzyna Zamara. The Authors wish to thank Milegate Extension Landfill Management for their support, which made the project possible. Special thanks are due to Scott Hodges from Sandsfield Gravel Ltd for technical support. The authors also wish to thank GeoFabrics Ltd and VEOLIA Environmental Services Ltd for providing geomembrane and geotextile materials respectively and to the Environment Agency England and Wales for their support of the trial. Finally thanks are due to Dr Steve James and his researchers at Cranfield University for developing and installing the fibre optic strain measurement system.

REFERENCES

Akpinar, M.,V., Benson, C.H., 2005. Effect of temperature on shear strength of two geomembrane-geotextile interfaces. Geotextiles and Geomembranes, v 23, issue 5, October 2005, pages 443-453.

Arab, M., 2011, The Integrity of Geosynthetic Elements of Waste Containment Barrier Systems Subject to Seismic Loading. PhD thesis, Arizona State University. July 2011.

Cadwallader, M., Cranston, M., Peggs, I.D., 1993. White surfaced HDPE geomembranes: assessing their significance to liner design and installation. Proceedings of geosynthetics ’93, vol. 2, pp. 1065-1079.

565 Dixon, N., Jones, D. R., 2003. *Stability of Landfill Lining Systems: Report no.2 Guidance.*
566 Environment Agency Research and Development Technical Report P1-385/TR2.

567 Dixon, N., Jones, D. R., 2005. Engineering properties of municipal solid waste. *Geotextiles and*
568 *Geomembranes* 23, pp. 205-233.

569 Dixon, N., Jones, D.R.V. , Fowmes, G.J., 2006. Interface shear strength variability and its use in
570 reliability-based landfill stability analysis. *Geosynthetics International*. Vol. 13, No1. p 1.

571 Dixon, N., Zamara, K.A., Jones, D.R.V., Fowmes, G., 2012. Waste/Lining System Interaction:
572 Implications for Landfill Design and Long-term Performance. *Geotechnical Engineering Journal*
573 *of the SEAGS & AGSSEA* Vol. 43 No.3 September 2012 ISSN 0046-5828.

574 Ehrenber, H., Recker, C., 2012. The influence of Geosynthetics Color on the UV resistance
575 performance under natural and lab testing conditions. 5th European Geosynthetics Congress.
576 Valencia 2012. Proceedings Vol. 5. Topic: Mining & Environmental Applications.

577 Filz, G.M., Esterhuizen, J.J.B., Duncan, J.M., 2001. Progressive failure of lined waste
578 impoundments. Journal of Geotechnical and Geoenvironmental Engineering. October 2001, pp.
579 841-848.

580 Fowmes, G.J., Jones, D.R.V., Dixon, N. 2005. Analysis of a landfill directive compliant steep
581 wall lining system. Proceedings 10th International Waste Management and Landfill Symposium,
582 Sardinia. pp369.

583 Fowmes, G.J., Dixon, N., Jones, D.R.V., 2007. Landfill Stability and Integrity Toolbox. Internal
584 Golder Associates (UK) Ltd Design Guidance Document.

585 Fowmes, G.J., Dixon, N., Jones, D.R.V., 2008. Validation of a numerical modelling technique
586 for multilayered geosynthetic landfill lining systems. *Geotextiles and Geomembranes* 26, pp.
587 109–121.

588 Giroud, J.P., Morel, N., 1992. Analysis of geomembrane wrinkles. Geotextiles and
589 Geomembranes, 11, 1992, pp. 255-276

590 Gudina, S. and Brachman, R.W.I., 2011. Geomembrane strains from wrinkle deformation.

591 Jones, D.R.V., Dixon, N., 2005. Landfill lining stability and integrity: the role of waste
592 settlement. *Geotextiles and Geomembranes* 23, pp. 27-53.

593 Koerner, R. M., 2005. Designing with Geosynthetics, 5th Edition. Prentice Hall, Englewood Cliffs, NJ,
594 USA, 816 pp.

595

596 Koerner, R.M., Hsuan, Y., Lord, A.E., Jr., 1993. Remaining technical barriers to obtaining
597 general acceptance of geosynthetics, Geomembranes and Geotextiles, vol. 21, no. 1, pp. 1-53.

598 Koerner, R.M., Soong, T-Y. 2000. Stability Assessment of 10 Large Landfill Failures *Geodenver*
599 *2000 ASCE SPECIA* vol 103, pp. 1-38.

600 Lodi, P.C, de Souza Bueno, B., Zornberg, J.G., de Souza Correia, 2008. Analysis of mechanical
601 properties on geotextiles after weathering exposure. Conference proceedings EuroGeo4 paper no
602 203.

603 Muhsiung, C., 2005. Three-dimensional stability analysis of the Kettleman Hills landfill slope
604 failure based on observed sliding-block mechanism. Computers and Geotechnics 32, pp. 587–
605 599.

606 Peltie, T., Pierson, P., Gourc, J.P., 1994. Thermal analysis of geomembrane exposed to solar
607 radiation. Geosynthtetic international, vol. 1, no. 1, pp. 21-44.

608 Sia, A, Dixon, N., 2012. Numerical modelling of landfill lining system–waste interaction:
609 implications of parameter variability. Geosynthetics International, Volume 19, Issue 5, 01
610 October 2012 , pages 393 –408 , ISSN: 1072-6349, E-ISSN: 1751-7613

611 Sheirs, J., 2009. A guide to Polymeric Geomembranes: A practical approach. John Wiley &
612 Sons. ISBN 978-0-470-51920-2

613 Take, W.A., Watson, E., Brachman, R.W.I., Rowe, R.K., 2012. Thermal expansion and
614 contraction of geomembrane liners subjected to solar exposure and backfilling. Journal of
615 Geotechnical and Geoenvironmental Engineering.

616 Villard, P., Gourc, J.P., Feki, N., 1999. Analysis of geosynthetic lining system (GLS) undergoing
617 large deformations. Geotextiles and Geomembranes, Volume 17, Issue 1 February 1999, pp. 17-
618 32.

619 WunderGround, 2012. Web site accessed on 01/06/2012:
620 http://www.wunderground.com/weatherstation/WXDailyHistory.asp?ID=IEASTYOR11&day=6
621 &year=2010&month=5&graphspan=year

622 Zamara, K.A., Dixon, N., Jones, D.R.V., Fowmes, G., 2012. Monitoring of a landfill side slope
623 lining system: Instrument selection, installation and performance. Geotextiles and
624 Geomembranes, 35 (2012) pp.1-13.

625 Figure 1. Milegate Extension Landfill – the slope view 2010 and 2012, location of the slope and
626 basic geometry (after Zamara *et al.* 2012).

627

628

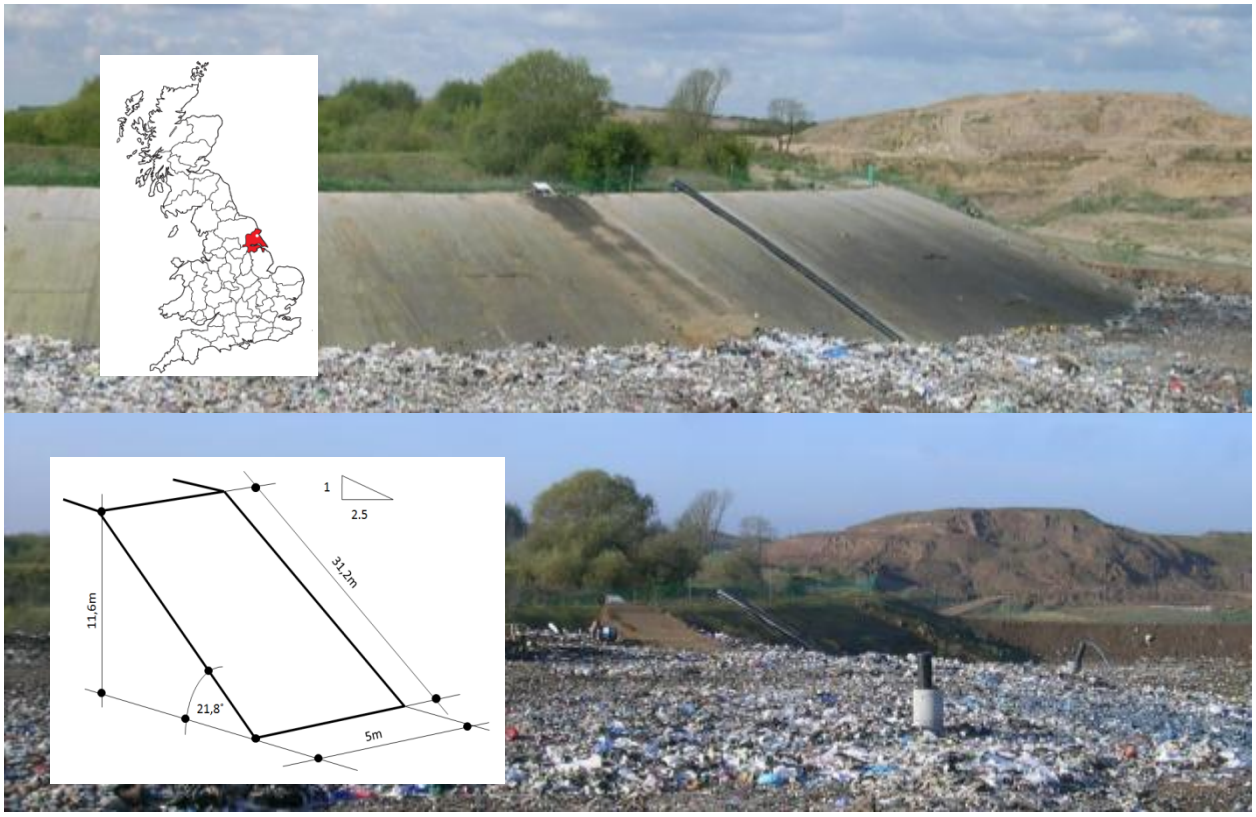

629

630 Figure 2. Multilayered side slope lining system – schematic view.

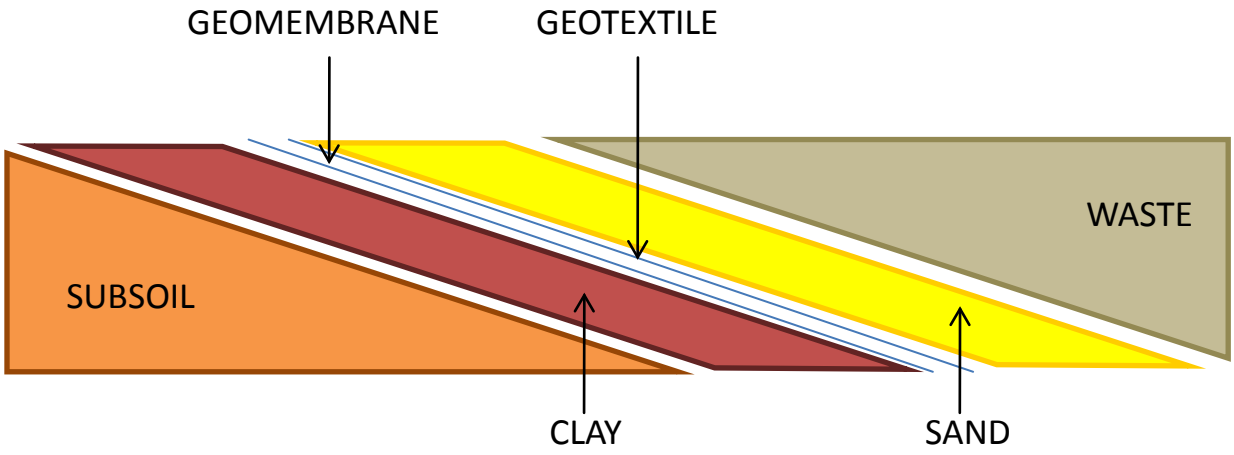

631

Figure 3. Instrument locations on the slope test panel – schematic view (after Zamara *et al.* 2012).

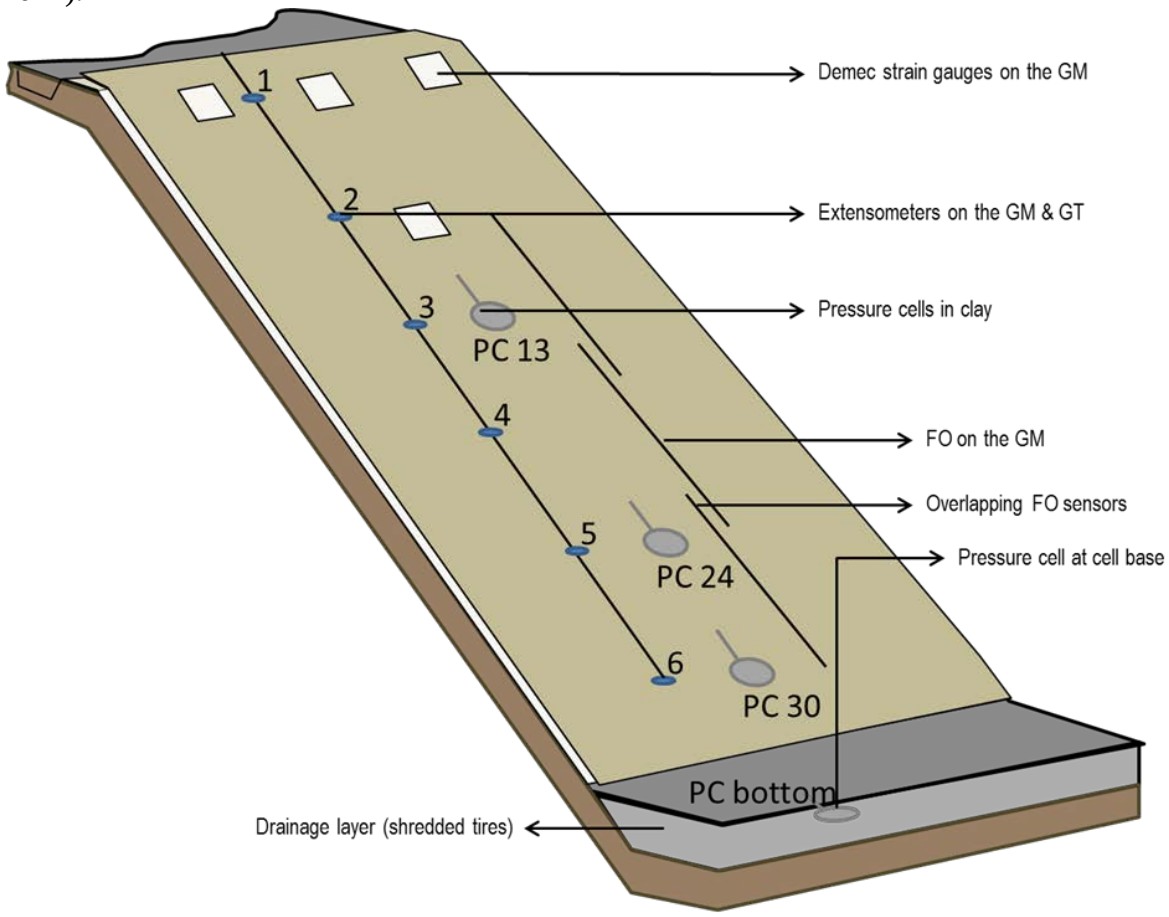

Figure 4. Measured pressures on the liner from sand veneers and waste (pressure cells) and computed values. All the values measured and computed are plotted correspondingly to the on-site instrument locations (left hand Y-axis represents slope length from the crest to the toe (0-31.2m), X- time axes are located in the relevant site instrument locations along the slope, right hand Y axis – represents waste height above toe of slope with the corresponding plot of the slope waste coverage).

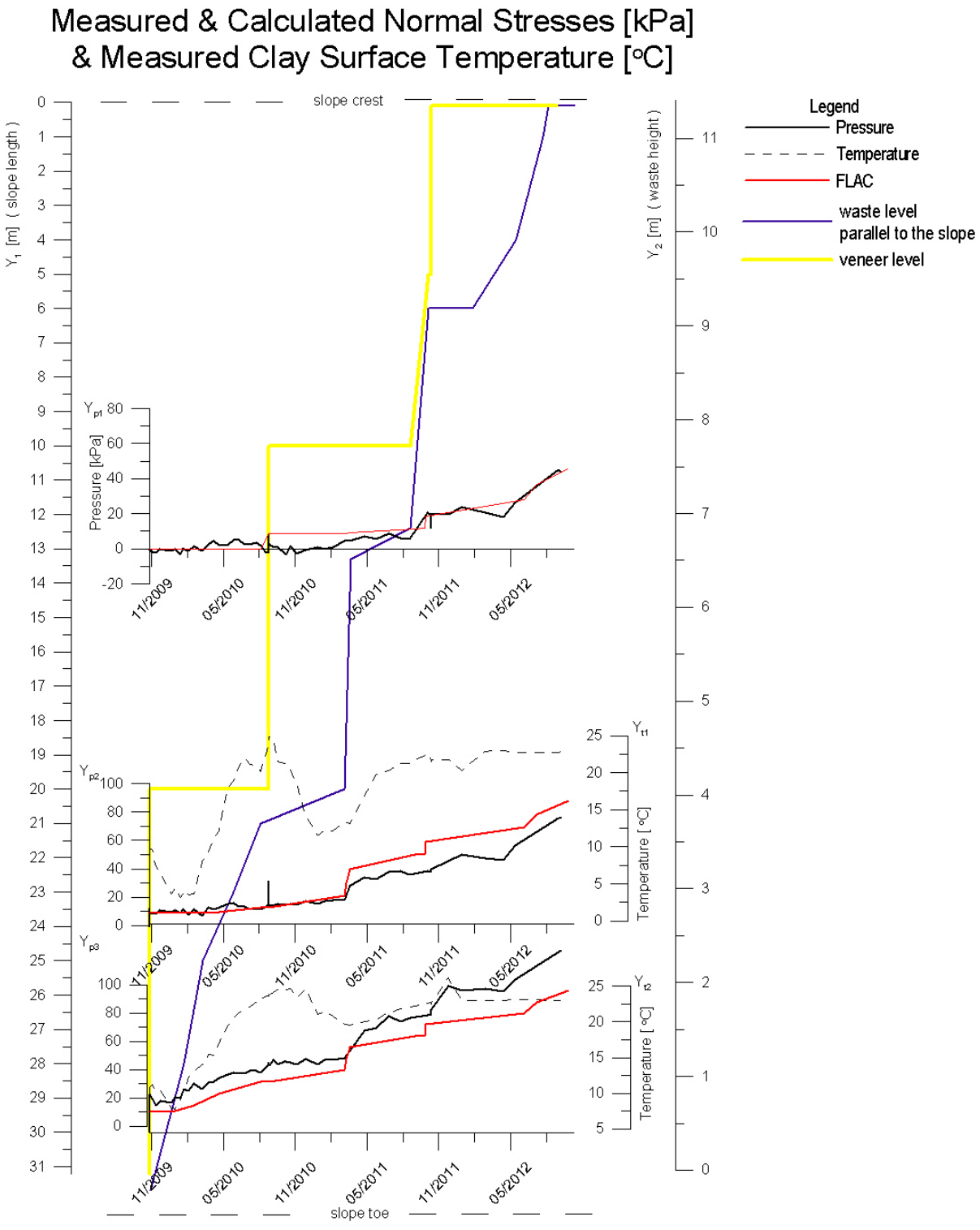
Measured & Calculated Normal Stresses [kPa]
& Measured Clay Surface Temperature [°C]
slope crest
slope toe
Y1 [m] (slope length)
Y2 [m] (waste height)
Pressure [kPa]
Temperature [°C]
11/2009
05/2010
11/2010
05/2011
11/2011
05/2012
Legend
Pressure
Temperature
FLAC
waste level
parallel to the slope
veneer level

641

642 Figure 5. Extensometer readings with plots presented in the same manner as Figure 4.
643 Extensometer locations on the slope are reflected on the left hand side axis, which represents
644 slope length starting from the crest measured parallel to the slope (i.e. each X axis is positioned
645 at the measuring point along the slope). Displacements of each pair of extensometers
646 (geomembrane and geotextile) are plotted on a relevant X- axis, with the same direction of the
647 movement (up or down the slope) as occurred on the slope. Results from FLAC numerivcal
648 analyses are also shown for comparison.
649

650

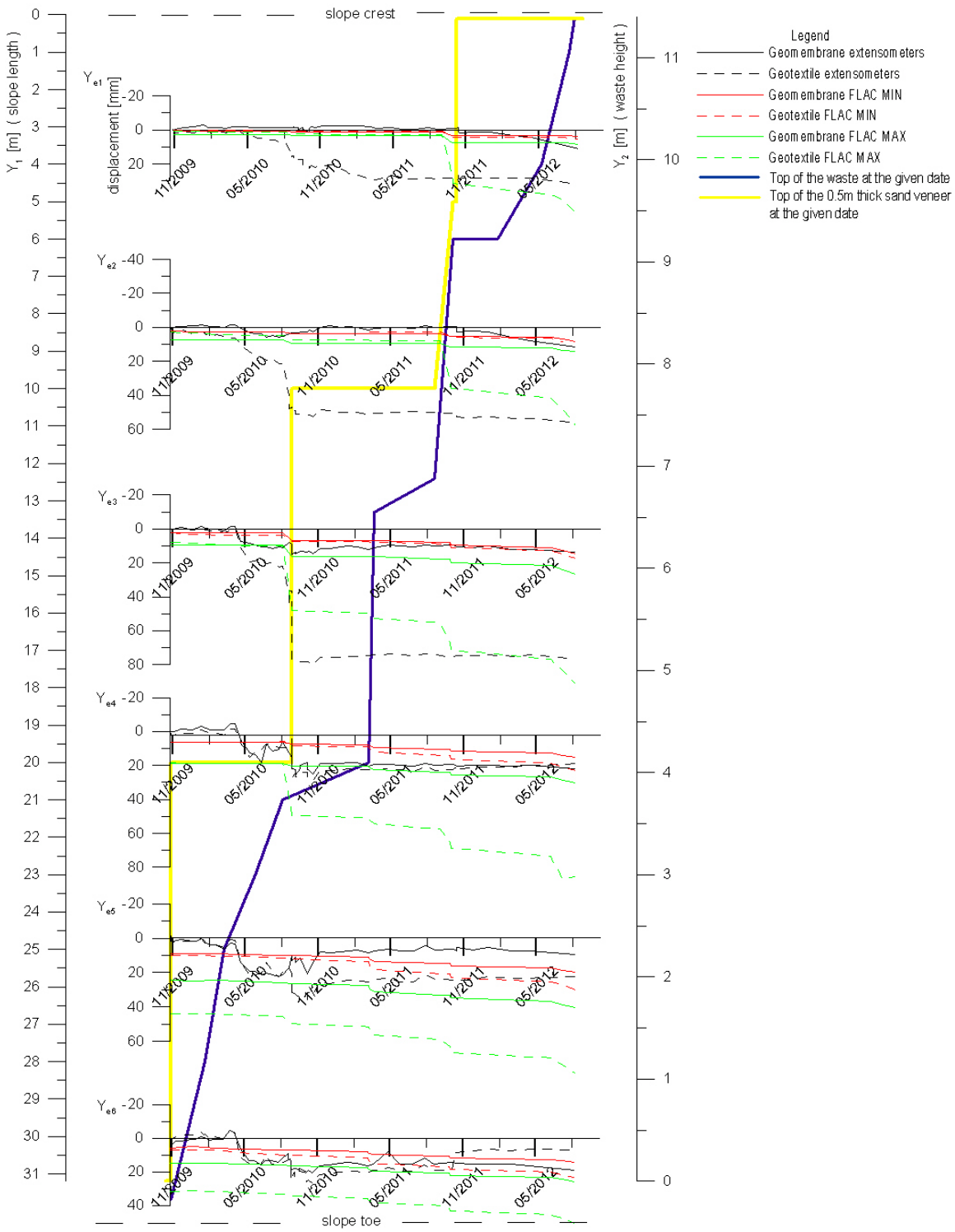
Geomembrane & Geotextile Extensometers
Measured & Computed Displacements [mm]
slope crest
slope toe
Y1 [m] (slope length)
Y2 [m] (waste height)
displacement [mm]
Ye1
Ye2
Ye3
Ye4
Ye5
Ye6
11/2009
05/2010
11/2010
05/2011
11/2011
05/2012
Legend
Geomembrane extensometers
Geotextile extensometers
Geomembrane FLAC MIN
Geotextile FLAC MIN
Geomembrane FLAC MAX
Geotextile FLAC MAX
Top of the waste at the given date
Top of the 0.5m thick sand veneer at the given date

651

652

Figure 6. Extensometer displacement measurements compared to displacements from selected numerical model analyses for the geomembrane and geotextile during staged construction at the following locations: a) 8.4m below the crest, b) 13.8m below the crest, c) 24.6m below the crest.

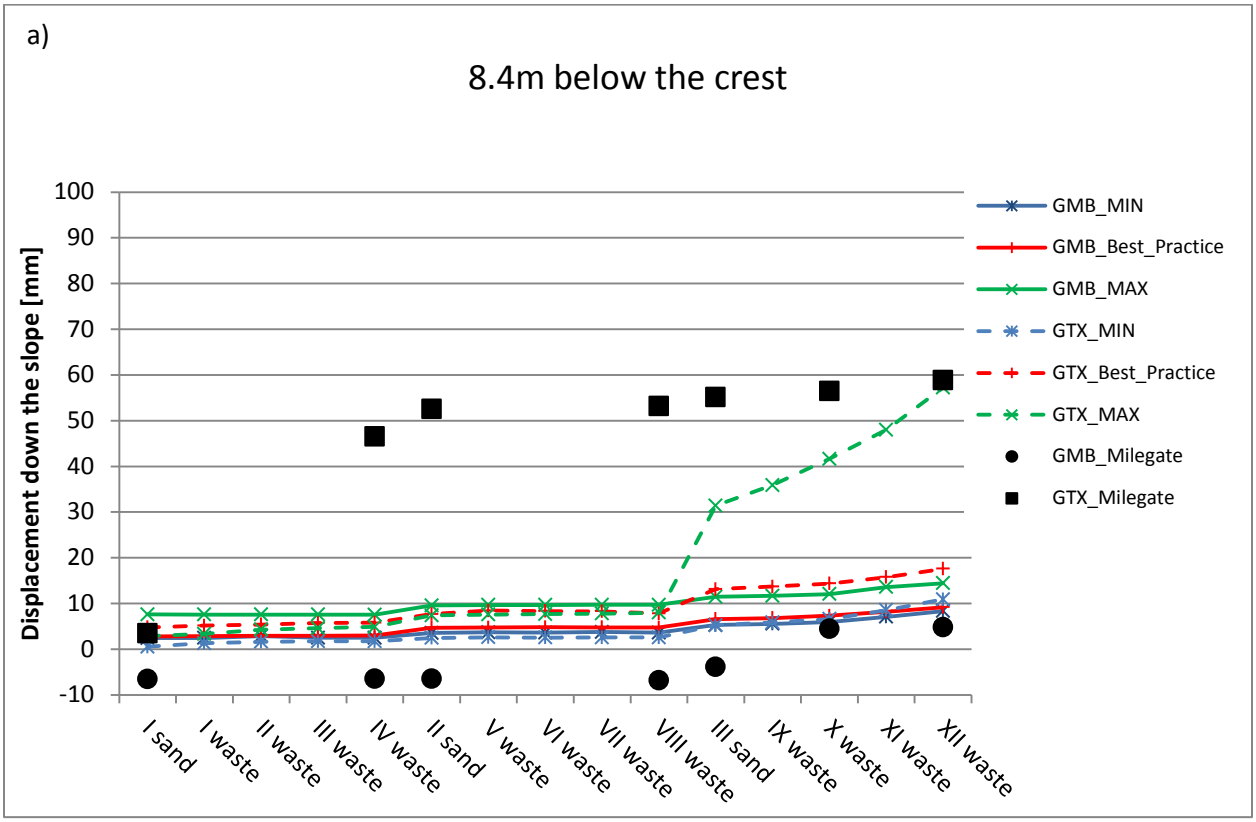

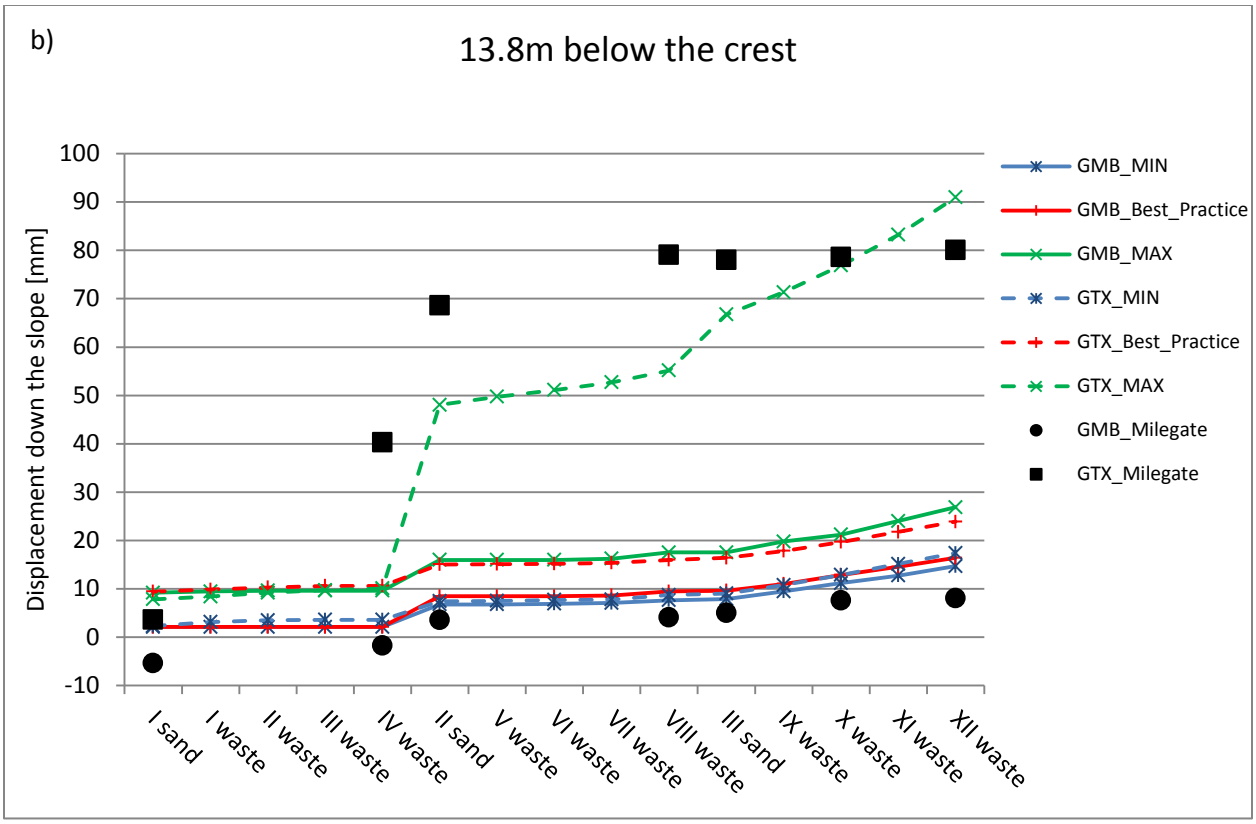
b)
13.8m below the crest
Displacement down the slope [mm]
100
90
80
70
60
50
40
30
20
10
0
-10
I sand
I waste
II waste
III waste
IV waste
II sand
V waste
VI waste
VII waste
VIII waste
III sand
IX waste
X waste
XI waste
XII waste
GMB_MIN
GMB_Best_Practice
GMB_MAX
GTX_MIN
GTX_Best_Practice
GTX_MAX
GMB_Milegate
GTX_Milegate

658

659

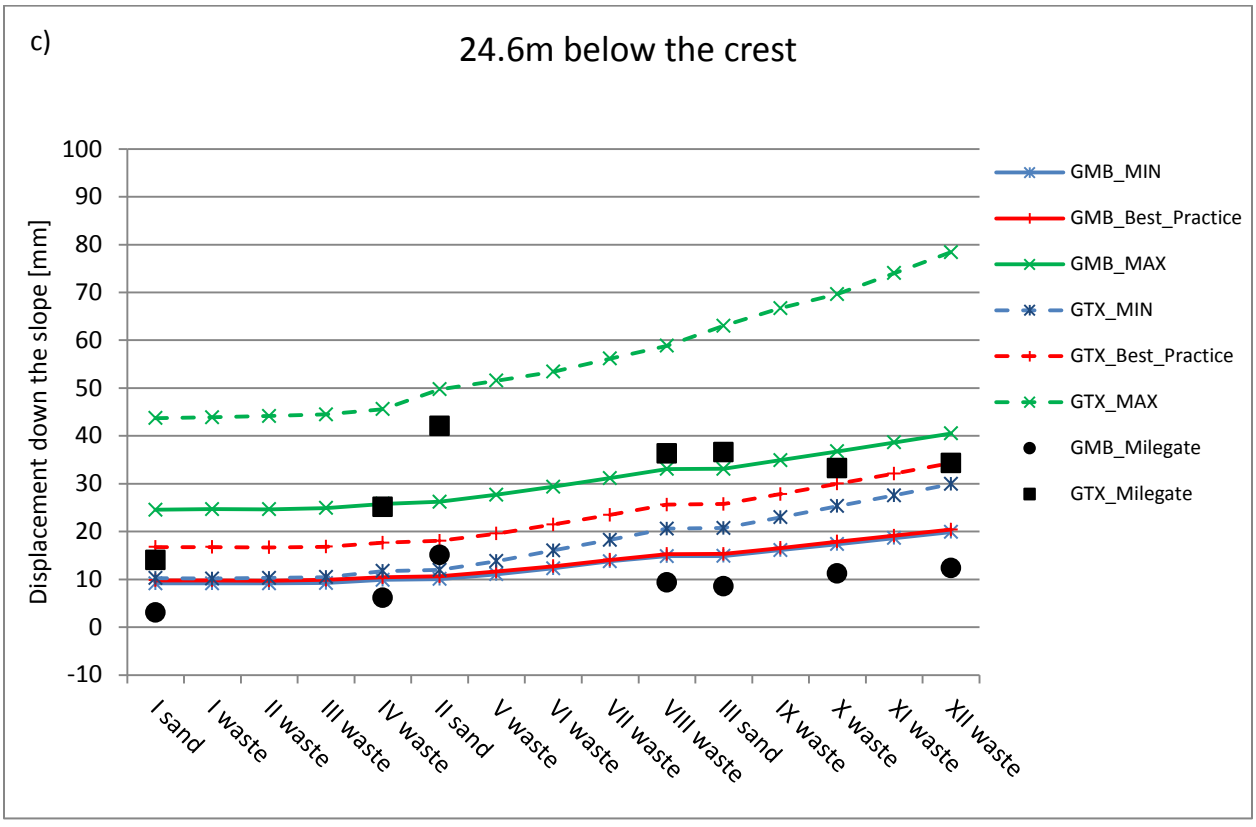
c)
24.6m below the crest
Displacement down the slope [mm]
100
90
80
70
60
50
40
30
20
10
0
-10
I sand
I waste
II waste
III waste
IV waste
II sand
V waste
VI waste
VII waste
VIII waste
III sand
IX waste
X waste
XI waste
XII waste
GMB_MIN
GMB_Best_Practice
GMB_MAX
GTX_MIN
GTX_Best_Practice
GTX_MAX
GMB_Milegate
GTX_Milegate

660

Figure 7. Comparison of measured and computed displacements following completion of waste filling

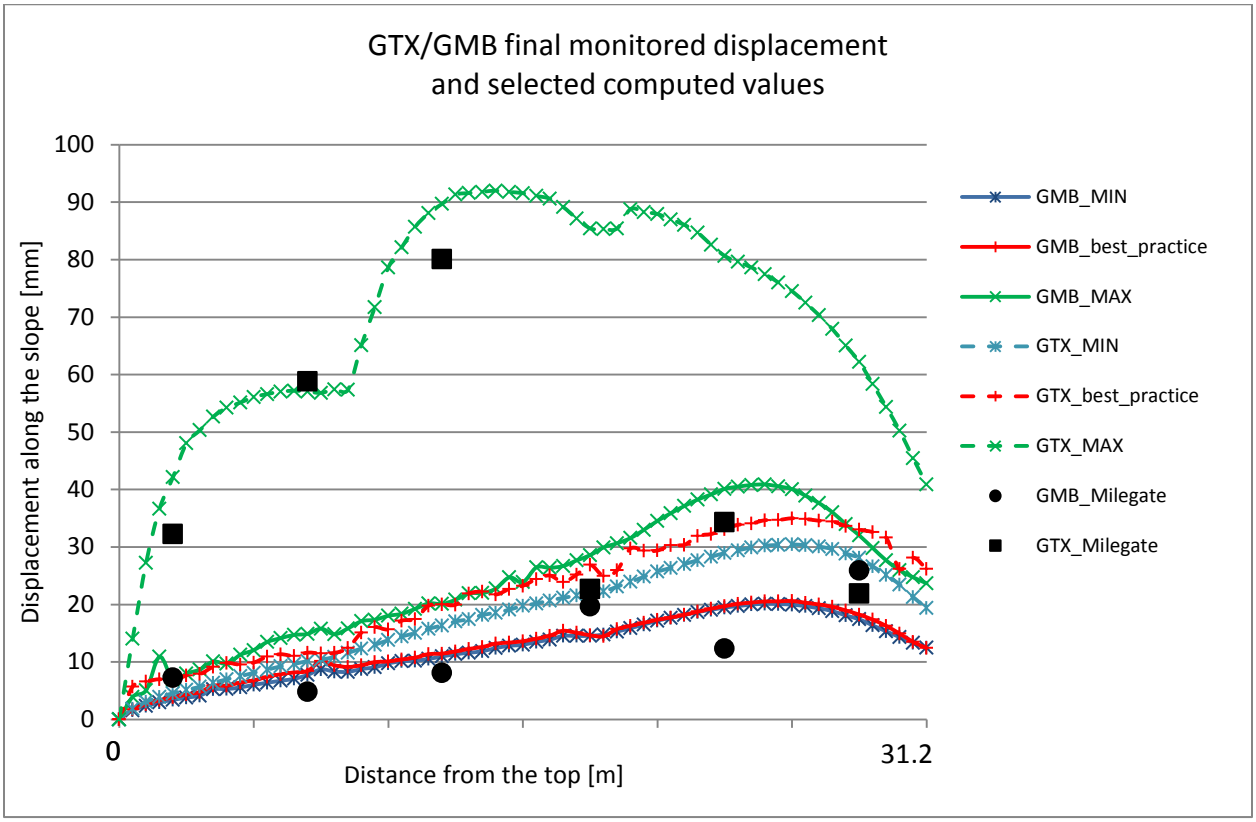

667 Figure 8. Comparison of measured and computed geomembrane strains: a) after placement of the

668 1st veneer, b) prior to placement of the 2nd veneer, and c) following completion of waste filling.

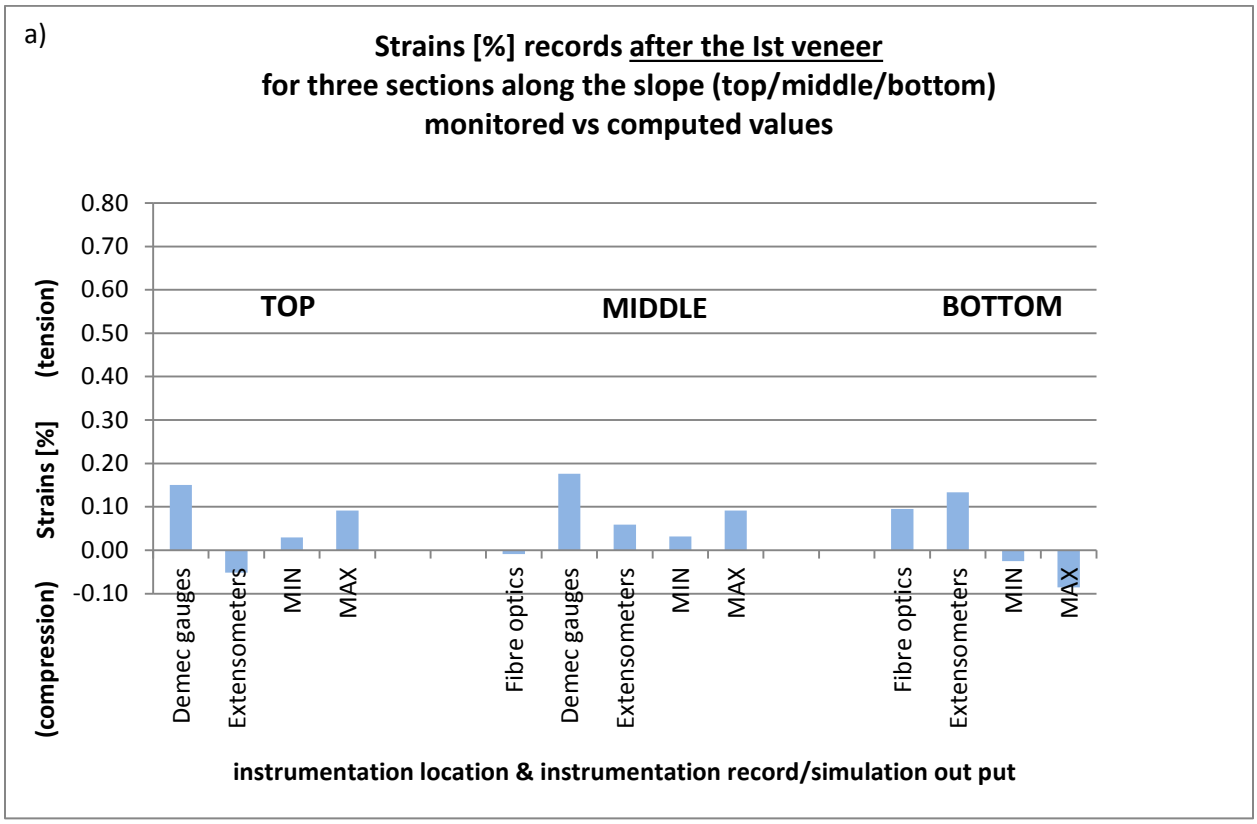

669

670

671

b)

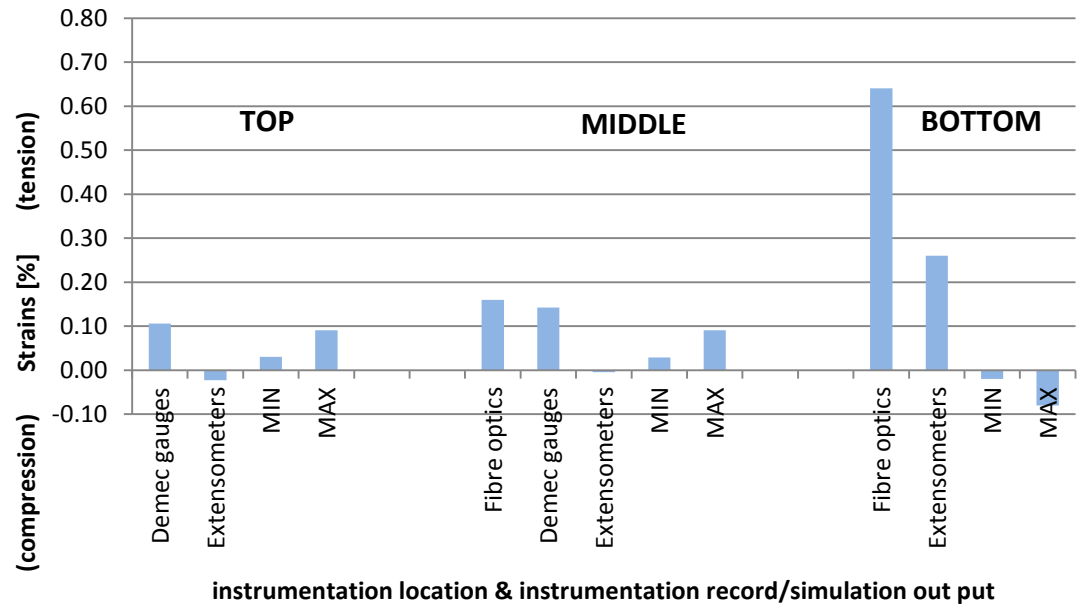
Strains [%] records prior to the II veneer
for three sections along the slope (top/middle/bottom)
monitored vs computed values
0.80
0.70
0.60
0.50
0.40
0.30
0.20
0.10
0.00
-0.10
(compression) Strains [%] (tension)
TOP
MIDDLE
BOTTOM
Demec gauges
Extensometers
MIN
MAX
Fibre optics
Demec gauges
Extensometers
MIN
MAX
Fibre optics
Extensometers
MIN
MAX
instrumentation location & instrumentation record/simulation out put

672

c)

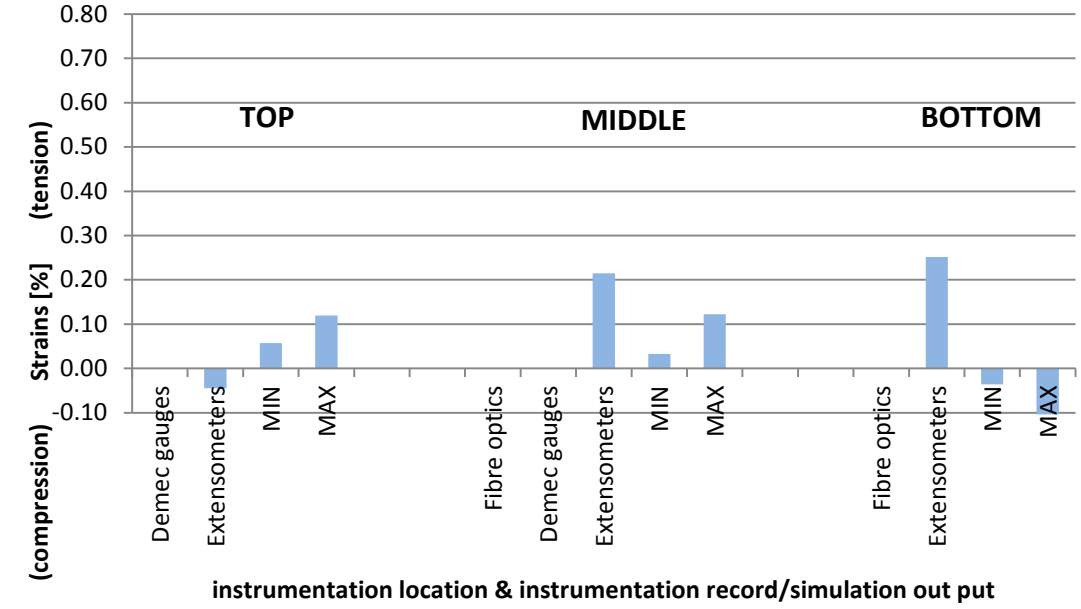
Strains [%] records FINAL STAGE
for three sections along the slope (top/middle/bottom)
monitored vs computed values
0.80
0.70
0.60
0.50
0.40
0.30
0.20
0.10
0.00
-0.10
(compression) Strains [%] (tension)
TOP
MIDDLE
BOTTOM
Demec gauges
Extensometers
MIN
MAX
Fibre optics
Demec gauges
Extensometers
MIN
MAX
Fibre optics
Extensometers
MIN
MAX
instrumentation location & instrumentation record/simulation out put

673

674 Figure 9. Temperatures measured on the top surface of the geomembrane, beneath the geotextile

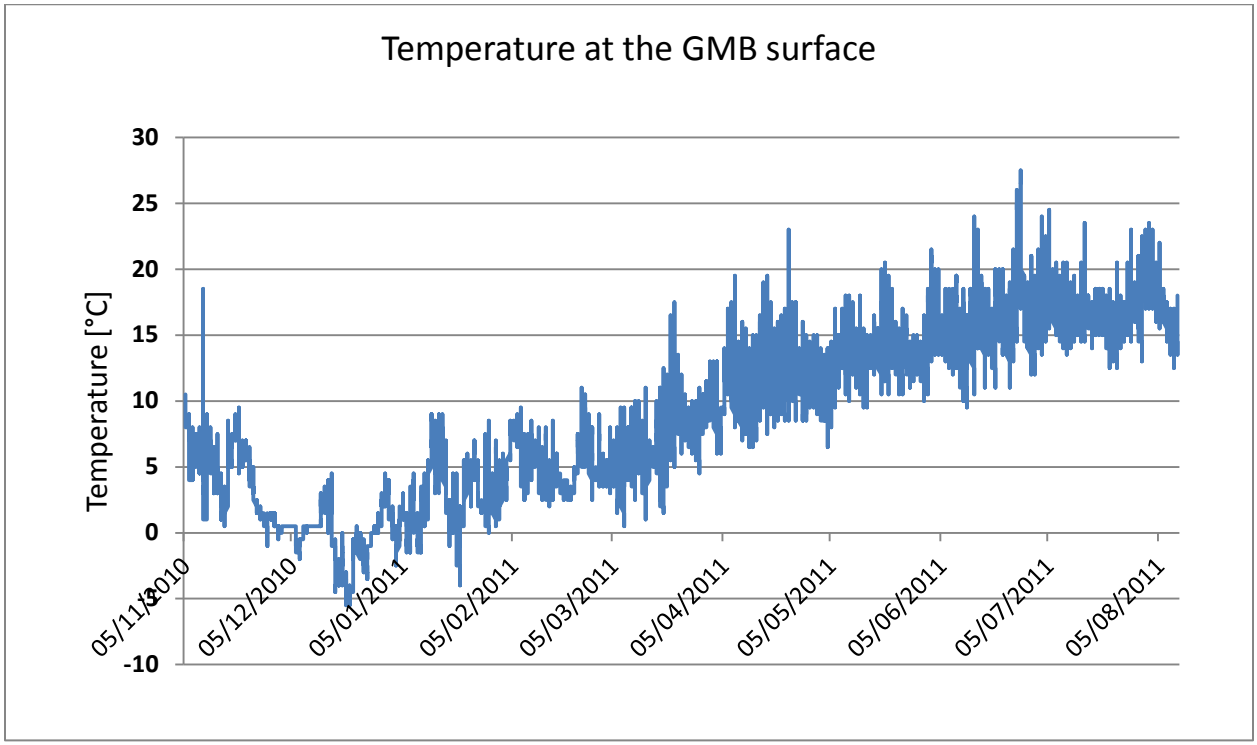

675

676 Figure 10. Geomembrane Demec strain gauge measurements for locations at the top of and

677 across the slope.

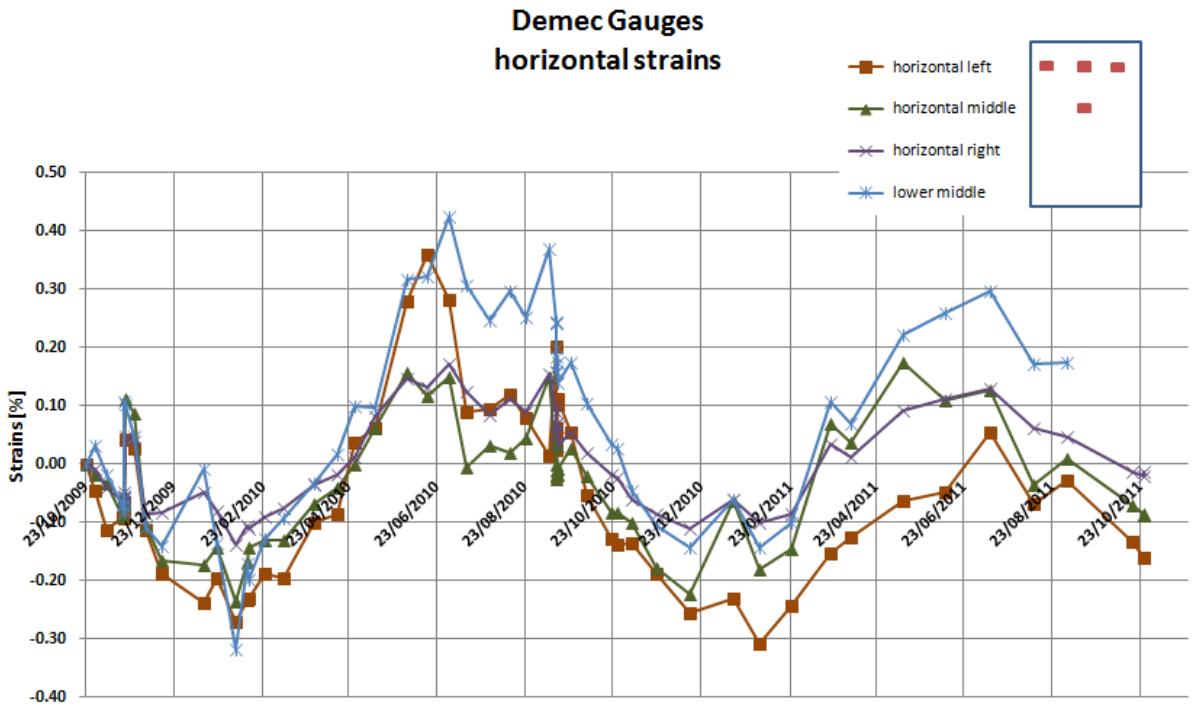

678

679

Figure 11. Wrinkles in the geotextile with the contracted, planar, geomembrane beneath taken on 07/09/2010.

685 Figure 12. Schematic geotextile deformation of exposed lining system in response to a cycle of

686 temperature

687

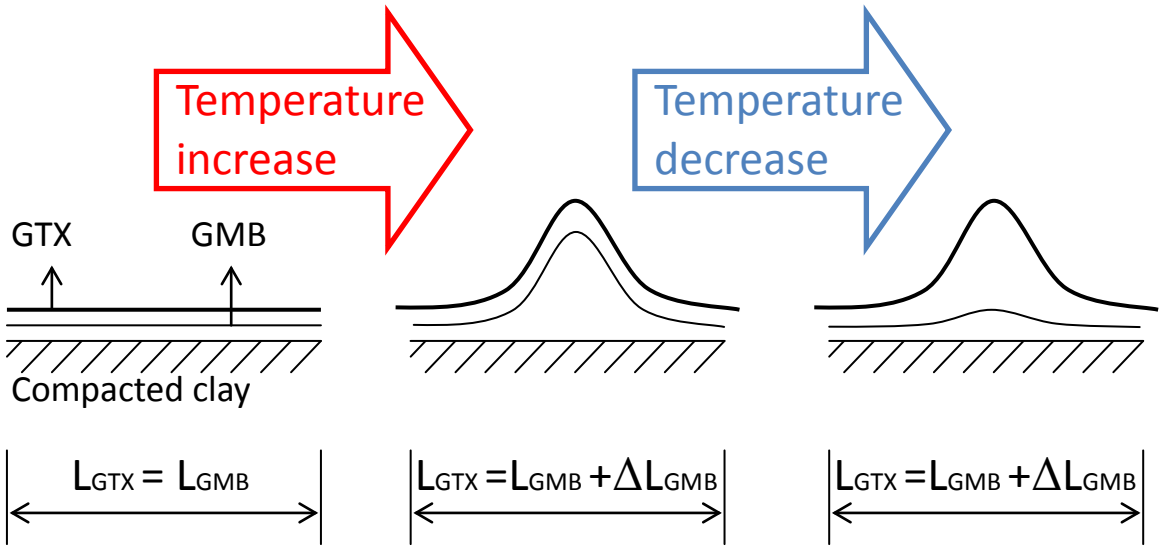

688

689

690 Table 1. Instruments and parameters measured at Milegate Extension Landfill.

Instrument	Number of instruments / sensors	Measured parameter
Vibrating Wire Pressure Cells	4	Normal Stress
Extensometers	12	Displacement (at 6 points on the GM, 6 on the GT)
Demec strain gauges	16 steel disks	GM strains across the slope
		GM strains along the slope
Fibre Optics	15	GM strains along the slope
	7	GM temperature
Thermistors	2	Clay surface temperature
Additional records		Waste height
Temperature logger	1	GM temperature

691

692

693

694

695

696 Table 2. Material properties for FLAC model analysis.

697

Material	Model	Density (Mg/m^3)	φ' (°)	c' (kPa)	Young's Modulus (MPa)	Poisson's Ratio
Waste	Mohr - Coulomb	1.0	25	5	0.5	0.3
Sand layer	Mohr - Coulomb	1.7	35	0	70 20*	0.4
Clay liner	Mohr - Coulomb	1.7	23	5	150 50*	0.3

698 699 700 701 702

703 *altered values in further simulation (see Table 4 for details).

704 Table 3. Interface properties used in modelling.

Interface	**δ (°) Peak/Residual**	**α (kPa) Peak/Residual**	**Normal stiffness (kPa/m)**	**Shear stiffness (kPa/m)**
Waste/sand	20	5	10000	5000
Sand/HPS			10000	4500
dry	29.9/29.6	6.3/1.8		
wet	29.6/29.9	3.2/1.3		
HPS/HDPE			10000	4500
dry	19.9/13.3	2.3/1.4		
wet	20.8/14.7	4.0/2.9		
HDPE/Clay			10000	5500
drained	22.0/22.0	8.0/8.0		
undrained	31.1/25.1	7.6/3.2		

705

706 Table 4. Model outputs and measured values for geomembrane and geotextile displacements and

707 strains

IN-PUT VALUES COMBINATIONS			**RESULTS**			
Applied interface shear strength	**Clay Stiffness [MPa]**	**Soil/Geotextile Stiffness [MPa]**	**Geotextile Max Displacements [mm]**	**Geomembrane Max Displacements [mm]**	**Geomembrane Max Strains [%]**	**Geomembrane Max Axial Forces [kN/m]**
Peak	**150**	**70/1.2**	**30.5**	**20.1**	0.13	1.13
Strain Softening			**35.3**	**20.7**	**0.18**	**1.59**
Reduced values	**50**	**20/1.8**	**92.0**	**40.9**	0.26	2.29
Measuring instruments			**Monitored values**			
Extensometers readings			**83.5**	**25.9**	0.26	1.76
Demec gauge slope direction*			-	-	0.31	2.09
Demec gauge across slope direction*			-	-	0.42	2.83
Fibre optic readings*			-	-	0.78	5.27

708

709 *Demec gauge and Fibre optic readings are suspected to be mostly temperature related; this is
710 based on the time when the readings were collected and section on the slope where the reported
711 peak occurred.

712 Table 5. Deformation of the geotextile during placement of the 2nd sand veneer obtained from
713 extensometer readings compared to theoretical elongation of the geomembrane sheet for the
714 exposed section. Theoretical elongation are calculated for the lower boundary assuming
715 $\Delta T=30°C$ and coefficient of thermal expansion equal $1.1x10^{-4}$ cm/cm/°C, and higher boundary
716 $\Delta T=40°C$ and coefficient of thermal expansion equal $1.5x10^{-4}$ cm/cm/°C.

Sensor ID	Sensor location below the crest / When covered by the sand layer	**Monitored** geotextile **displacement** during placement of the 2nd sand veneer	**Theoretical geomembrane elongation** due to temp. change for the exposed HDPE sheet length
Ext.1	3.0 m 1st veneer	20 mm	9.9 - 18.0 mm
Ext.2	8.4 m 2nd veneer	50 mm	27.7 - 50.4 mm
Ext.3	13.8 m 3rd veneer	80 mm	45.5 - 82.8 mm

717

718

719